C05
Proceedings of the 5th International Conference on Inverse Problems in Engineering: Theory and Practtice, Cambridge, UK, 11-15th July 2005

REGULARIZED BEM SOLUTION FOR INVERSE BOUNDARY VALUE PROBLEMS IN ANISOTROPIC ELASTICITY

L. COMINO[1], L. MARIN[2] and R. GALLEGO[1]
[1] *Department of Structural Mechanics, University of Granada, Politécnico de Fuentenueva, 18071 Granada, Spain*
E-mails: lcomino@ugr.es, gallego@ugr.es
[2] *School of Mechanical, Materials, Manufacturing Engineering and Management, The University of Nottingham, University Park, Nottingham NG7 2RD, UK*
E-mail: liviu.marin@nottingham.ac.uk

Abstract. This communication deals with an alternating iterative algorithm proposed by Kozlov *et al.* [6] for obtaining approximate solutions to the ill-posed Cauchy problem. In particular, the application to anisotropic elasticity is analysed, whilst the boundary element method (BEM) is used for the numerical implementation. The numerical results confirm that the iterative BEM produces a convergent and stable numerical solution with respect to increasing the number of boundary elements and decreasing the amount of noise added into the input data.

1. INTRODUCTION

In solving physical problems in solid mechanics one usually deals with direct problems, but sometimes one or more of the conditions for solving them are not available. Therefore an *inverse problem* may be formulated to determine the unknowns from specified or measured system responses. It is well known that inverse problems are in general unstable, see e.g. Hadamard [1], and hence a suitable algorithm is required in order to solve them. The Cauchy problem in elasticity, in which both the displacement and the traction vectors are known on a part of the boundary and no data are available on the remaining boundary, is a classical example of an inverse problem in solid mechanics. There are important studies in the literature for solving the problem for isotropic elastic materials, many of them based on the FEM, see e.g. Maniatty *et al.* [2] and Schnur and Zabaras [3], and lately, using BEM techniques, see e.g. Marin *et al.* [4, 5]. Also methods of obtaining an approximate solution to ill-posed boundary value problems have been discussed extensively, *iterative methods* being the most recently developed. These have two main advantages, namely they allow any physical constraint and they have a computational scheme very simple to be implemented as a sequence of well-posed problems. Based on these reasons, in this study we have used the BEM in order to implement a convergent algorithm for anisotropic linear elastic materials. It consists of an alternating iterative procedure which solves successive well-posed mixed boundary value problems. It was originally proposed by Kozlov *et al.* [6] and then implemented for isotropic linear elastic solids by Marin *et al.* [4, 5].

2. MATHEMATICAL FORMULATION OF THE CAUCHY PROBLEM IN TWO-DIMENSIONAL ANISOTROPIC ELASTICITY

Consider an anisotropic linear elastic homogeneous solid $\Omega \subset \mathbb{R}^3$ bounded by a smooth surface Γ in the sense of Liapunov, such that $\Gamma = \Gamma_1 \cup \Gamma_2$, where $\Gamma_1, \Gamma_2 \neq \emptyset$ and $\Gamma_1 \cap \Gamma_2 = \emptyset$. In particular, we consider the case when the geometry and the loading conditions describe a pure plane strain state. Therefore, the problem can be simplified to a two-dimensional study. In the presence of body forces $\mathbf{b}$, the equilibrium equations of the elastic medium are given by, see e.g. Lekhnitskii [7],

$$\operatorname{div}(\boldsymbol{\sigma}(\mathbf{u})) + \mathbf{b} = 0 \quad \text{in} \quad \Omega, \tag{1}$$

where $\boldsymbol{\sigma}$ is the stress tensor. On assuming small deformations only, the strain tensor $\boldsymbol{\varepsilon}$ is defined by the following kinematic relations:

$$\boldsymbol{\varepsilon} = \frac{1}{2}\left(\nabla \mathbf{u} + \nabla^T \mathbf{u}\right) \quad \text{in} \quad \Omega, \tag{2}$$

is related to the stress tensor $\boldsymbol{\sigma}$ by Hooke's constitutive law, namely

$$\boldsymbol{\sigma} = \mathbf{C} : \boldsymbol{\varepsilon} \quad \text{in} \quad \Omega, \tag{3}$$

where $\mathbf{C}$ is the elasticity tensor of order four. In two-dimensional anisotropic linear elastic solids, the constitutive relation (3) is usually expressed using a mono-index notation [1]

$$\sigma_i = c_{ij}\varepsilon_j, \qquad \varepsilon_i = a_{ij}\sigma_j, \qquad i,j = 1,\dots 6, \tag{4}$$

where ε_j is the strain tensor, c_{ij} is the elasticity tensor and a_{ij} is the compliance tensor.

Direct problems are solved taking into account equations $(1)-(3)$, together with the knowledge of the displacement and/or the traction vectors on the entire boundary Γ. It should be mentioned that analytical solutions can be found only for a limited number of cases, i.e. for simple geometries and boundary conditions. Then, if the complex potential theory [7] is used, the anisotropic linear elastic problem can be expressed in terms of the complex potentials $\Phi_i(z_i) = F_i'(z_i)$, where the stress function $F(x_1, x_2)$ has been introduced as

$$F(x_1, x_2) = \Re[F_1(z_1) + F_2(z_2)] + F_0(x_1, x_2). \tag{5}$$

Here $F_i(z_i)$, $i = 1, 2$, are two arbitrary analytical functions of the complex variables $z_i = x_1 + \mu_i x_2$ and F_0 is a particular solution of the field equations. The complex parameters μ_i are always two conjugate pairs, roots of the characteristic fourth degree polynomial equation

$$\beta_{11}\mu^4 - 2\beta_{16}\mu^3 + (\beta_{12} + \beta_{66})\mu^2 - 2\beta_{16}\mu + \beta_{22} = 0, \tag{6}$$

where β_{ij} are called the reduced elastic constants whose values are given by $\beta_{ij} = a_{ij}$ for the plane stress state and $\beta_{ij} = a_{ij} - (a_{i3}a_{j3})/a_{33}$ for the plane strain state.

The following general expressions for stresses and displacements, respectively, can be obtained if no body forces are acting on the anisotropic solid:

$$\sigma_1 = 2\Re[\mu_1^2\Phi_1' + \mu_2^2\Phi_2'], \quad \sigma_2 = 2\Re[\Phi_1' + \Phi_2'], \quad \sigma_6 = -2\Re[\mu_1\Phi_1' + \mu_2\Phi_2'] \tag{7}$$

$$u_1 = 2\Re[p_{11}\Phi_1 + p_{12}\Phi_2] - \omega x_2 + u_0, \quad u_2 = 2\Re[p_{21}\Phi_1 + p_{22}\Phi_2] + \omega x_1 + v_0 \tag{8}$$

where u_0, v_0 and ω represent a simultaneous rigid-body motion and the material parameters p_{ik}, $i,k = 1, 2$, are given by

$$p_{1k} = \beta_{11}\mu_k^2 + \beta_{12} - \beta_{16}\mu_k, \quad p_{2k} = \beta_{12}\mu_k + \frac{\beta_{22}}{\mu_k} - \beta_{26}, \quad k = 1, 2. \tag{9}$$

If it is possible to measure both the displacement and traction vectors on a part of the boundary Γ, say $\Gamma_2 \subset \Gamma$, and there is no information on the remaining boundary $\Gamma_1 = \Gamma \setminus \Gamma_2$ then this leads to the mathematical formulation of an inverse problem consisting of the equilibrium equation (1) (for simplicity, in the absence of body forces, i.e. $\mathbf{b} = 0$) and the given overspecified boundary conditions on Γ_2, namely

$$\begin{cases} \operatorname{div}(\boldsymbol{\sigma}(\mathbf{u})) = 0 & \text{in} \quad \Omega \\ \mathbf{u} = \widetilde{\mathbf{u}} & \text{on} \quad \Gamma_2 \\ \mathbf{t} = \widetilde{\mathbf{t}} & \text{on} \quad \Gamma_2. \end{cases} \tag{10}$$

Here $\widetilde{\mathbf{u}}$ and $\widetilde{\mathbf{t}}$ are prescribed vector valued displacements and tractions, respectively. The Cauchy problem is much more difficult to solve since its solution does not satisfy the general conditions of well-posedness and hence regularization must be employed in order to solve stably this inverse problem. Therefore, knowing the exact data $\widetilde{\mathbf{u}}$ and $\widetilde{\mathbf{t}}$ on the boundary Γ_2, we use a convergent iterative regularizing algorithm, originally proposed by Kozlov *et al.* [6] and implemented for isotropic linear elastic media by Marin *et al.* [4, 5].

3. DESCRIPTION OF THE ALGORITHM

In this communication, the approach proposed for solving the Cauchy problem is based on a convergent iterative algorithm. It was proposed by Kozlov *et al.* [6] for Cauchy problems associated to linear, elliptic, self-adjoint and positive-definite operators. This algorithm consists of the following steps:

Step 1.1. Set $k = 0$. Specify an initial approximation $\boldsymbol{t}^{(0)}$ for the tractions on the underspecified boundary Γ_1.

[1] $11 \to 1, \quad 22 \to 2, \quad 33 \to 3, \quad 23 \to 4, \quad 13 \to 5, \quad 12 \to 6$

Step 1.2. Solve the mixed boundary value problem

$$\begin{cases} \operatorname{div}\left(\boldsymbol{\sigma}\left(\boldsymbol{u}^{(1)}\right)\right)=0 & \text{in} \quad \Omega \\ \boldsymbol{t}^{(1)} \equiv \boldsymbol{\sigma}\left(\boldsymbol{u}^{(1)}\right) \cdot \boldsymbol{n}=\boldsymbol{t}^{(0)} & \text{on} \quad \Gamma_1 \\ \boldsymbol{u}^{(1)}=\widetilde{\boldsymbol{u}} & \text{on} \quad \Gamma_2 \end{cases} \tag{11}$$

in order to determine the displacements $\boldsymbol{u}^{(1)}$ in Ω and on Γ_1.

Step 2.1. Having constructed the approximation $\boldsymbol{u}^{(2k-1)}$, $k>0$, the mixed boundary value problem

$$\begin{cases} \operatorname{div}\left(\boldsymbol{\sigma}\left(\boldsymbol{u}^{(2k)}\right)\right)=0 & \text{in} \quad \Omega \\ \boldsymbol{u}^{(2k)}=\boldsymbol{u}^{(2k)} & \text{on} \quad \Gamma_1 \\ \boldsymbol{t}^{(2k)} \equiv \boldsymbol{\sigma}\left(\boldsymbol{u}^{(2k)}\right) \cdot \boldsymbol{n}=\widetilde{\boldsymbol{t}} & \text{on} \quad \Gamma_2 \end{cases} \tag{12}$$

is solved to determine the displacements $\boldsymbol{u}^{(2k)}$ in Ω and the tractions $\boldsymbol{t}^{(2k)} \equiv \boldsymbol{\sigma}\left(\boldsymbol{u}^{(2k)}\right) \cdot \boldsymbol{n}$ on Γ_1.

Step 2.2. Having constructed the vector-valued function $\boldsymbol{u}^{(2k)}$, $k>0$, the mixed boundary value problem

$$\begin{cases} \operatorname{div}\left(\boldsymbol{\sigma}\left(\boldsymbol{u}^{(2k+1)}\right)\right)=0 & \text{in} \quad \Omega \\ \boldsymbol{t}^{(2k+1)} \equiv \boldsymbol{\sigma}\left(\boldsymbol{u}^{(2k+1)}\right) \cdot \boldsymbol{n}=\boldsymbol{t}^{(2k)} & \text{on} \quad \Gamma_1 \\ \boldsymbol{u}^{(2k+1)}=\widetilde{\boldsymbol{u}} & \text{on} \quad \Gamma_2 \end{cases} \tag{13}$$

is solved in order to determine the displacements $\boldsymbol{u}^{(2k+1)}$ in Ω and on Γ_1.

Step 3. Set $k=k+1$ and repeat steps 2.1 and 2.2 until a prescribed stopping criterion is satisfied.

Kozlov *et al.* [6] showed that if Γ is smooth, the alternating algorithm based on steps $1-3$ produces two sequences of approximate solutions $\left\{\boldsymbol{u}^{(2k)}(\boldsymbol{x})\right\}_{k>0}$ and $\left\{\boldsymbol{u}^{(2k-1)}(\boldsymbol{x})\right\}_{k>0}$ which both converge to the solution $\boldsymbol{u}(\boldsymbol{x})$ of the Cauchy problem (10) for any initial guess $\boldsymbol{t}^{(0)}$. The same conclusion is obtained if at the step 1.1 we specify an initial guess $\boldsymbol{u}^{(0)}$ and we modify accordingly the steps 1 and 2 of the algorithm. Problems $(11)-(13)$ are well-posed and solvable using a numerical approach. Passing from one iteration to the next, only the values of the displacement and traction vectors on the boundary Γ are required. If we also take into account that the BEM performs better than domain discretisation methods, such as the finite difference method (FDM) and the FEM, for problems with linear partial differential equations [8] then the BEM is the most suitable numerical technique for solving the intermediate mixed boundary value problems.

4. THE BOUNDARY ELEMENT METHOD (BEM)

The BEM is based on the boundary integral representation of the displacements. This technique is derived from Betti's Reciprocity Theorem applied to the actual elastostatic state in the domain Ω and an auxiliary field called the fundamental solution.

4.1. Fundamental solution

The fundamental solution is the response of a system at a point $\mathbf{z}$ due to a point load applied at $\mathbf{z}'$ in an infinite domain with the same material properties as the original problem. When a unit load is applied in the x_i-direction, the solution is given by the complex potential, see e.g. Sollero [9],

$$\Phi_{is}(z_s)=A_{is}\ln(z_s-z_s') \tag{14}$$

where A_{is} are complex constants. These constants can be computed by employing the system of equations obtained from the implementation of the boundary conditions, namely

$$\begin{pmatrix} 1 & -1 & 1 & -1 \\ \mu_1 & -\bar{\mu}_1 & \mu_2 & -\bar{\mu}_2 \\ p_{11} & -\bar{p}_{11} & p_{12} & -\bar{p}_{12} \\ p_{21} & -\bar{p}_{21} & p_{22} & -\bar{p}_{22} \end{pmatrix} \begin{pmatrix} A_{i1} \\ \bar{A}_{i1} \\ A_{i2} \\ \bar{A}_{i2} \end{pmatrix} = \begin{pmatrix} \dfrac{\delta_{i2}}{2\pi i} \\ \dfrac{\delta_{i1}}{2\pi i} \\ 0 \\ 0 \end{pmatrix} \tag{15}$$

The fundamental solution for the displacements is obtained in the following form:

$$U_{ij}(\mathbf{z},\mathbf{z}') = 2\sum_{s=1}^{2} \Re\left[p_{js}A_{is}\ln\left(z_s - z_s'\right)\right], \tag{16}$$

while the corresponding fundamental tractions on the boundary are given by

$$T_{ij}(\mathbf{z},\mathbf{z}') = 2\sum_{s=1}^{2} \Re\left[\frac{q_{js}A_{is}}{z_s - z_s'}\left(\mu_1 n_1 - n_2\right)\right], \tag{17}$$

where $q_{1s} = \mu_s$, $q_{2s} = -1$ and n_i are the components of the outward normal vector $\mathbf{n}$ at Γ.

4.2. Boundary integral equation

Once the auxiliary state is defined, we recall Betti's Reciprocity Theorem which is applied to two balanced systems of boundary and body forces $(\mathbf{t},\mathbf{b})$ and $(\mathbf{t}^*,\mathbf{b}^*)$. These systems of forces are applied to the same anisotropic elastic domain characterised by the displacement fields $\mathbf{u}$ and $\mathbf{u}^*$, respectively. If the $*$ state is the one given by the fundamental solution then

$$b_j^* = \delta_{ij}\,\delta(\mathbf{z}-\mathbf{z}'), \quad t_j^* = T_{ij}(\mathbf{z},\mathbf{z}'), \quad u_j^* = U_{ij}(\mathbf{z},\mathbf{z}'), \tag{18}$$

where δ_{ij} is the Kronecker delta tensor, δ is the Dirac delta distribution and $\mathbf{z}'$ is a point inside the solution domain Ω. On assuming that no body forces act on the solid, i.e. $\mathbf{b} = 0$ in (1), then Somigliana identity is obtained as

$$u_i(\mathbf{z}') + \int_\Gamma T_{ij}(\mathbf{z},\mathbf{z}')u_j(\mathbf{z})\;d\Gamma = \int_\Gamma U_{ij}(\mathbf{z},\mathbf{z}')t_j(\mathbf{z})\;d\Gamma. \tag{19}$$

By moving $\mathbf{z}'$ to the limit to boundary point $\mathbf{y}\in\Gamma$, i.e. $\mathbf{z}'\to\mathbf{y}$ we obtain the boundary integral equation (BIE) which governs the elastic displacement field and is given by

$$c_{ij}(\mathbf{y})u_j(\mathbf{y}) + \int_\Gamma T_{ij}(\mathbf{z},\mathbf{y})u_j(\mathbf{z})\;d\Gamma = \int_\Gamma U_{ij}(\mathbf{z},\mathbf{y})t_j(\mathbf{z})\;d\Gamma, \tag{20}$$

where the free term $c_{ij}(\mathbf{y})$ depends on the location of the collocation point $\mathbf{z}'$, see París and Cañas [8].

Finally, on differentiating equation (19) with respect to the coordinates of the collocation point $\mathbf{z}'\in\Omega\setminus\Gamma$ then the integral equation for the strains is obtained as

$$\epsilon_{ik}(\mathbf{z}') = \int_\Gamma V_{ijk}(\mathbf{z},\mathbf{z}')t_j(\mathbf{z})\;d\Gamma - \int_\Gamma S_{ijk}(\mathbf{z},\mathbf{z}')u_j(\mathbf{z})\;d\Gamma. \tag{21}$$

For details on the computation of the new kernels V_{ijk} and S_{ijk}, we refer the reader to [10].

4.3. Discretisation of the problem

In order to solve numerically the BIE (20), the boundaries Γ, Γ_1 and Γ_2 are discretised into N_e, N_e^1 and N_e^2 elements, respectively, such that $N_e^1 + N_e^2 = N_e$. The geometry, displacements and stresses are interpolated over each element using their values at the nodes and some shape functions ϕ_m. For every collocation point l with the coordinates $\mathbf{y}^l$ the BIE (20) can be written in discretised form as

$$c_{ij}u_j(l) + \sum_{k=1}^{N_e}\sum_{m=1}^{3} h_{ij}^m(l,k)u_j^k(m) = \sum_{k=1}^{N_e}\sum_{m=1}^{3} g_{ij}^m(l,k)t_j^k(m), \tag{22}$$

where the integration constants $h_{ij}^m(l,k)$ and $g_{ij}^m(l,k)$, $i,j=1,2$, $m=1,2,3$, are given by

$$h_{ij}^m(l,k) = \int_{-1}^{1} T_{ij}(\mathbf{z}(\xi),\mathbf{y}^l)\phi_m(\xi)J^k(\xi)\;d\xi, \qquad g_{ij}^m(l,k) = \int_{-1}^{1} U_{ij}(\mathbf{z}(\xi),\mathbf{y}^l)\phi_m(\xi)J^k(\xi)\;d\xi. \tag{23}$$

In this study, isoparametric quadratic elements have been used such that if the boundary Γ is closed and is discretised into N_e elements then the total number of boundary nodes is given by $N = 2N_e$. Consequently, the numbers of boundary nodes corresponding to the underspecified Γ_1 and overspecified Γ_2 boundaries are given by $N_1 = 2N_e^1$ and $N_2 = 2N_e^2$, respectively, such that $N_1 + N_2 = N$. Integration

constants computation can be checked in [10].

On applying equation (22) for all the boundary nodes, we obtain the following system of linear algebraic equations:

$$\mathbf{HU} = \mathbf{GT}, \tag{24}$$

where $\mathbf{U}$ and $\mathbf{T}$ are vectors containing the nodal values of the displacements and tractions, respectively. The discretisation of the boundary conditions (10_2) and (10_3) provides the values of $4N_2$ of the unknowns and the problem reduces to solving a system of $2N$ equations with $4N_1$ unknowns which can be generically written as

$$\mathbf{CX} = \mathbf{F}, \tag{25}$$

where the matrix $\mathbf{C} \in \mathbb{R}^{2N \times 4N_1}$ depends solely on the geometry of the boundary and the material properties, the vector $\mathbf{X} \in \mathbb{R}^{4N_1}$ contains the unknown values of the displacements and the tractions on the boundary Γ_1 and the vector $\mathbf{F} \in \mathbb{R}^{2N}$ is computed using the Cauchy boundary conditions (10_2) and (10_3).

5. NUMERICAL RESULTS

In this section we illustrate the numerical results obtained using the alternating iterative algorithm presented in Section 3, in conjunction with the BEM described in Section 4. In addition, we investigate the convergence with respect to the mesh size discretisation and the number of iterations when the data are exact and the stability when the data are perturbed by noise.

5.1. Examples

Two test examples in a two-dimensional smooth geometry (a condition required by the theoretical analysis of Kozlov *et al.* [6]) are used to prove the performance of the numerical method proposed. The Cauchy problem is defined for an annular domain $\Omega = \left\{\mathbf{x} = (x_1, x_2) \,\middle|\, r_i^2 < x_1^2 + x_2^2 < r_o^2 \right\}$, $r_i = 1$, $r_o = 4$. We assume that the boundary Γ of the solution domain is divided into two disjointed parts, namely $\Gamma_1 = \Gamma_i \equiv \left\{\mathbf{x} \in \Gamma \,\middle|\, x_1^2 + x_2^2 = r_i^2 \right\}$ and $\Gamma_2 = \Gamma_o \equiv \left\{\mathbf{x} \in \Gamma \,\middle|\, x_1^2 + x_2^2 = r_o^2 \right\}$ in the case of Example 1, and $\Gamma_1 = \{\mathbf{x} \in \Gamma_i \,|\, \alpha_1 \leq \Theta(\mathbf{x}) \leq \alpha_2 \}$ and $\Gamma_2 = \Gamma_o \cup \{\mathbf{x} \in \Gamma_i \,|\, 0 \leq \Theta(\mathbf{x}) < \alpha_1 \} \cup \{\mathbf{x} \in \Gamma_i \,|\, \alpha_2 < \Theta(\mathbf{x}) \leq 2\pi \}$ in the case of Example 2, where $\Theta(\boldsymbol{x})$ is the angular polar coordinate of $\boldsymbol{x}$ and $\alpha_i, i = 1, 2$, are specified angles in the interval $(0, 2\pi)$. In order to illustrate the typical numerical results we have taken $\alpha_1 = \pi/4$ and $\alpha_2 = 3\pi/4$. In the following examples we consider an orthotropic linear elastic medium (birch plywood), whose material orthotropy axes coincide with the axes of the Cartesian reference system. The orthotropic solid considered in this study is characterised by the engineering elastic constants $E_1 = 11.76$ GN/m^2, $E_2 = 5.88$ GN/m^2, $G_{12} = 0.686$ GN/m^2 and $\nu_{12} = 0.071$ and hence the compliance elastic constants are given by $a_{11} = 0.08503$ m^2/GN, $a_{12} = -0.006037$ m^2/GN, $a_{22} = 0.1701$ m^2/GN, $a_{66} = 1.4577$ m^2/GN and $a_{16} = a_{26} = 0.0$ m^2/GN.

Example 1. We consider a stress state corresponding to constant internal and external pressures $\sigma_i = 1.0$ GN/m^2 and $\sigma_e = 2.0$ GN/m^2, respectively.

Example 2. We consider a uniform hydrostatic stress state given by $\sigma_e = 1.5$ GN/m^2.

Analytical expressions for the stresses $\boldsymbol{\sigma}^{(\mathrm{an})}$ and displacements $\mathbf{u}^{(\mathrm{an})}$ are not available in this case. However, these can be obtained numerically by solving a direct problem with a very fine mesh in order to obtain the best numerical approximations. Hence the Cauchy problem considered in this paper is described by equation (10) in which the Cauchy data are given by $\widetilde{\mathbf{t}} = \mathbf{t}^{(\mathrm{an})}$ and $\widetilde{\mathbf{u}} = \mathbf{u}^{(\mathrm{an})}$. In the sequel, the analytical traction vector $\mathbf{t}^{(\mathrm{an})}$ and the corresponding displacement vector $\mathbf{u}^{(\mathrm{an})}$ will be referred to as "exact" traction and displacement vectors, respectively. The Cauchy problems given by equation (10) for the examples considered in this study have been solved iteratively using the BEM to provide simultaneously the unspecified boundary displacement and traction vectors on the boundary Γ_1. The number of isoparametric quadratic boundary elements used for discretising the boundary Γ was taken to be $N_e \in \{32, 48, 96\}$ such that both the underspecified and the overspecified boundaries Γ_1 and Γ_2, respectively, were discretised into the same number of isoparametric quadratic boundary elements, namely $N_e/2 \in \{16, 24, 48\}$.

5.2. Initial guess

An arbitrary vector valued function $\mathbf{t}^{(0)}$ may be specified as an initial guess for the traction vector on Γ_1, but in order to improve the rate of convergence of the iterative procedure we have chosen a vector valued function which ensures the continuity of the traction vector at the endpoints of Γ_1 and which is

also linear with respect to the angular polar coordinate Θ. For the test Example 2, this initial guess is given by

$$\mathbf{t}^{(0)}(\mathbf{x}) = \frac{\alpha_2 - \Theta(\mathbf{x})}{\alpha_2 - \alpha_1}\mathbf{t}^{(0)}(\mathbf{x}_1) + \frac{\Theta(\mathbf{x}) - \alpha_1}{\alpha_2 - \alpha_1}\mathbf{t}^{(0)}(\mathbf{x}_2), \tag{26}$$

where $\alpha_i = \Theta(\mathbf{x}_i)$ for $i = 1, 2$, $\mathbf{x}_1$ and $\mathbf{x}_2$ are the endpoints of Γ_1, and the choice of $\alpha_1 = \pi/4$ and $\alpha_2 = 3\pi/4$ also ensures that the initial guess is not too close to the exact values $\mathbf{t}^{(\mathrm{an})}(\mathbf{x})$.

In the case of Example 1, we cannot use the procedure described above and, therefore, the initial guess has been chosen as

$$\mathbf{t}^{(0)}(\mathbf{x}) = 0. \tag{27}$$

5.3. Convergence of the algorithm

The convergence of the algorithm has been studied evaluating, at each iteration, the accuracy errors defined by

$$E_u = \|\mathbf{u}^{(k)} - \mathbf{u}^{(\mathrm{an})}\|_{L^2(\Gamma_1)\times L^2(\Gamma_1)}, \tag{28}$$

$$E_t = \|\mathbf{t}^{(k)} - \mathbf{t}^{(\mathrm{an})}\|_{L^2(\Gamma_1)\times L^2(\Gamma_1)}, \tag{29}$$

where $\mathbf{u}^{(k)}$ and $\mathbf{t}^{(k)}$ are the displacement and the traction vectors on the boundary Γ_1 retrieved after k iterations, respectively, and each iteration consists of solving the two mixed well-posed problems mentioned in Section 3. The error in predicting the displacement vector inside the solution domain Ω may also be evaluated by using the expression

$$E_\Omega = \|\mathbf{u}^{(k)} - \mathbf{u}^{(\mathrm{an})}\|_{L^2(\Omega)\times L^2(\Omega)}, \tag{30}$$

but it has an evolution similar to that of the errors E_u and E_t, since the displacement values inside the solution domain are retrieved from the values of the displacement $\mathbf{u}$ and traction $\mathbf{t}$ on the boundary Γ.

When starting with the initial guess $\mathbf{t}^{(0)}$ given by equations (27) and (26) for Examples 1 and 2,

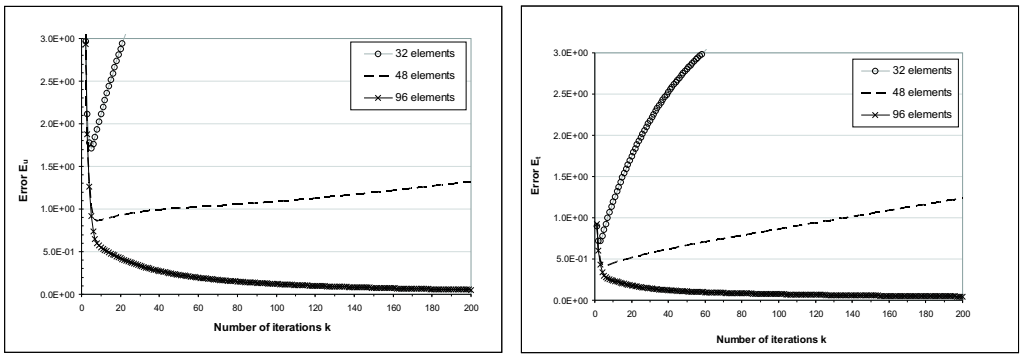

Figure 1: The accuracy errors E_u (left) and E_t (right), as functions of the number of iterations k, obtained using three different BEM meshes for the Example 1.

respectively, a sequence $\left\{\mathbf{u}^{(k)}\right\}_{k>0}$ of approximation functions for $\mathbf{u}|_{\Gamma_1}$ is obtained and, according to Kozlov *et al.* [6], this sequence converges to the exact solution. If we evaluate the errors E_u and E_t at every iteration, in the case of Example 1, then we note that both these errors keep decreasing with respect to increasing the number of iterations performed only for the finest BEM mesh, i.e. $N_e = 96$, see Figure 1. On the contrary, if the coarser BEM discretisations are used, i.e. $N_e = 32, 48$, then the accuracy errors given by expressions (28) and (29) attain a minimum value after a certain iteration number, k, after which they start increasing. However, the errors E_u and E_t corresponding to the Cauchy problem given by Example 2 have a decreasing tendency as k increases for all the BEM discretisations used. A possible explanation for the different behaviours of the accuracy errors E_u and E_t for Examples 1 and 2 is represented by the type of initial guess used for each of the Cauchy problems analysed. More precisely, the initial guess corresponding to Example 2 ensures the continuity of the traction vector at the endpoints of the underspecified boundary Γ_1, whereas the initial guess for the Example 1 is the constant vector zero which contains no information about the unknowns on Γ_1, see equations (26) and (27), respectively.

Figures 3 and 4 present the exact and the BEM numerical solutions for the displacement u_1 and the traction t_2 on the underspecified boundary Γ_1, obtained for the Cauchy problems given by Examples

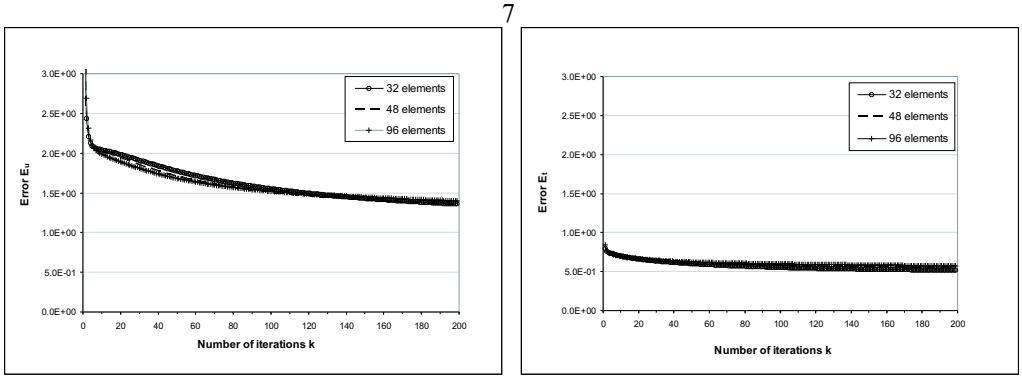

Figure 2: The accuracy errors E_u (left) and E_t (right), as functions of the number of iterations k, obtained with three different BEM discretisations for the Example 2.

1 and 2, respectively. From these figure it can be seen that the numerical results for both u_1 and t_2 retrieved for the Example 1 are more accurate than those corresponding to Example 2. The reason for this is that $\overline{\Gamma}_1 \cap \overline{\Gamma}_2 = \emptyset$ in the case of Example 1, whilst $\overline{\Gamma}_1 \cap \overline{\Gamma}_2 \neq \emptyset$ in the case of Example 2, i.e. there exist two points where the problem changes to mixed boundary conditions.

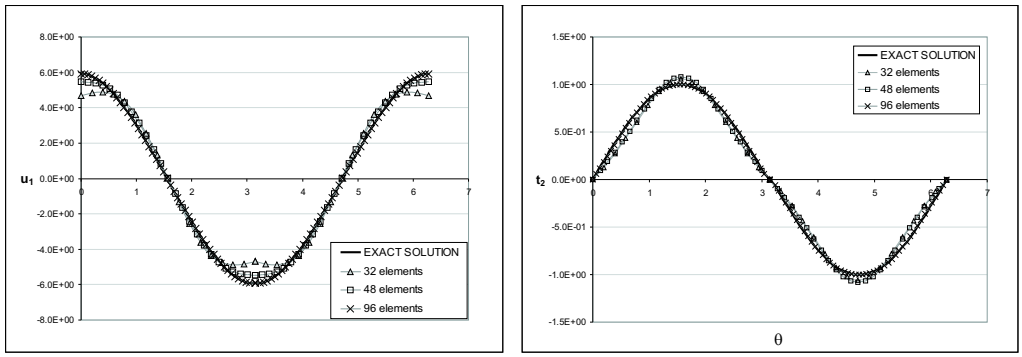

Figure 3: The exact and the numerical solutions for the displacement u_1 (left) and traction t_2 (right), obtained using various BEM discretisations for the Example 1.

5.4. Variable relaxation factor

The errors in predicting the traction $t_2|_{\Gamma_1}$ in the case of Example 2 are still large, especially for the elements close to the ends of the underspecified boundary Γ_1, see Figure 5. In order to save on both, computational time and computer storage, and to improve the results for the traction vector on the underspecified part of the boundary, we relax the marching condition (13) through the use of

$$\mathbf{t}^{(2k+1)} = \boldsymbol{\sigma}\left(\mathbf{u}^{(2k+1)}\right) \cdot \mathbf{n} = \rho \mathbf{t}^{(2k)} + (1-\rho)\mathbf{t}^{(2k-1)} \qquad \text{on} \quad \Gamma_1 \tag{31}$$

when passing from step 2.1 to step 2.2 of the algorithm described in Section 3, where ρ is a relaxation parameter to be prescribed.

By a thorough inspection of the numerical solution for the traction vector on Γ_1 obtained after various numbers of iterations without relaxation, we noticed that at the endpoints of the underspecified boundary the rate of convergence is higher than elsewhere on Γ_1. After a few iterations the numerical solution for the traction vector at the endpoints of Γ_1 approaches the exact solution and after that, as we increase the number of iterations, it deviates from the exact traction whilst elsewhere on Γ_1 the numerical traction still approaches the exact value. The high rate of movement of the numerical traction at the endpoints of Γ_1 in comparison with its rate of movement elsewhere on the underspecified boundary suggests the introduction of a variable relaxation factor $\rho = \rho\left(\Theta(\mathbf{x})\right)$ which is small at the endpoints of Γ_1 and has a maximum value, say A, in the middle of Γ_1. The variable relaxation factor was chosen as, see also Marin

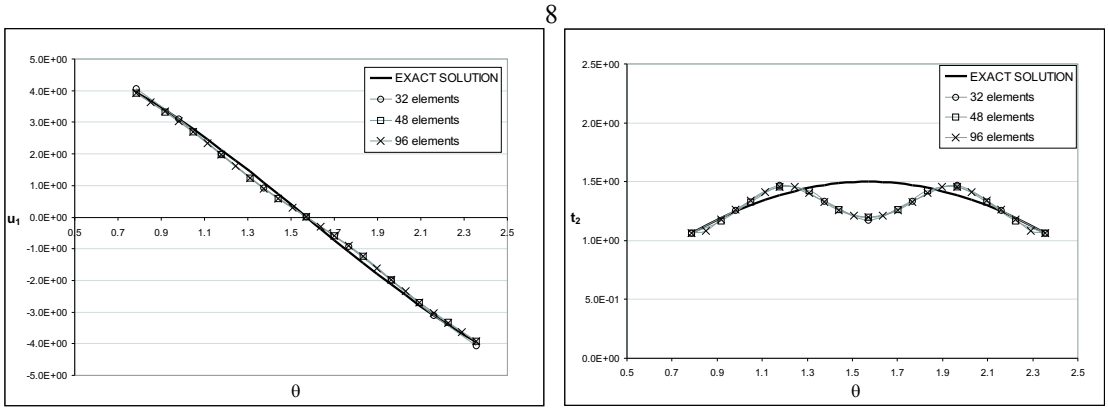

Figure 4: The exact and the numerical solutions for the displacement u_1 (left) and traction t_2 (right), obtained using various BEM discretisations for the Example 2.

et al. [4] and Mera *et al.* [11],

$$\rho\left(\Theta(\mathbf{x})\right) = A\sin\left(\frac{\Theta(\mathbf{x})-\alpha_1}{\alpha_2-\alpha_1}\,\pi\right), \tag{32}$$

where $A \in (0,2]$. Figure 5 illustrates more accurate estimates for the traction $t_2|_{\Gamma_1}$, obtained using the variable relaxation factor (31) with $A = 1.5$ although similar results can be obtained with $A \in (0,2]$.

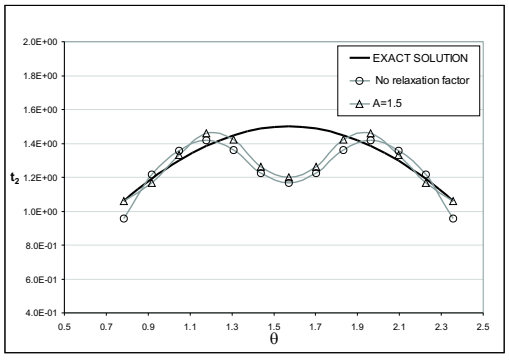

Figure 5: The exact and numerical solutions for the displacement $u_1|_{\Gamma_1}$, obtained using $N_e = 48$ elements in two cases, namely without relaxation factor and with a variable relaxation factor with amplitude A=1.5, for the Example 2.

5.5. Stopping criterion

Let the displacement vector on the overspecified boundary Γ_2 be perturbed as $\widetilde{u}_i|_{\Gamma_2} = u_i|_{\Gamma_2} + \delta u_i$, $i = 1,2$, where δu_i, $i = 1,2$, is a Gaussian random variable with mean zero and standard deviation $\sigma = \max_{\Gamma_2}|u_i| \times (p/100)$, $i = 1,2$, and p is the percentage of noise added into the input data $u_i|_{\Gamma_2}$. In Figure 6 we present the accuracy errors E_u and E_t corresponding to Example 1 for various levels of noise, namely $p \in \{1,3,5\}$. It can be seen from this figure that both errors E_u and E_t decrease up to a certain number of iterations, after which they start increasing. If the process is continued beyond this point then the numerical solutions lose their smoothness and become highly oscillatory and unbounded. Therefore, a regularizing stopping criterion must be used in order to cease the iterative process at the point where the errors in the numerical solutions start increasing.

If we evaluate the Euclidean norm of the vector $\mathbf{CX} - \mathbf{F}$ then this should tend to zero as $\mathbf{X}$ tends to the exact solution. Hence after each iteration we evaluate the error

$$k \in \mathbb{N}: \qquad E = \|\mathbf{C}\mathbf{X}^{(k)} - \mathbf{F}\|_2 \tag{33}$$

where $\mathbf{X}^{(k)}$ is a vector containing the components of the displacement and traction vectors on the underspecified boundary Γ_1 retrieved after k iterations. The error E includes information on both the

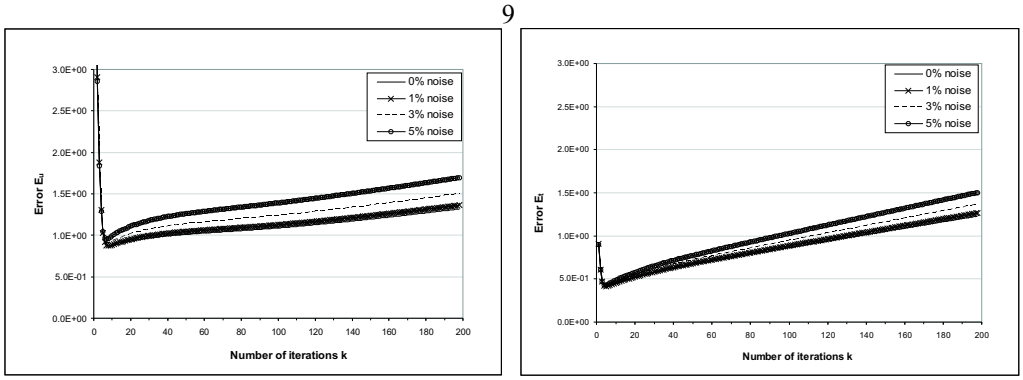

Figure 6: The accuracy errors E_u (left) and E_t (right), as functions of the number of iterations k, obtained using $N_e = 48$ and several amounts of noise added into the input data $\mathbf{u}|_{\Gamma_2}$, for the Example 1.

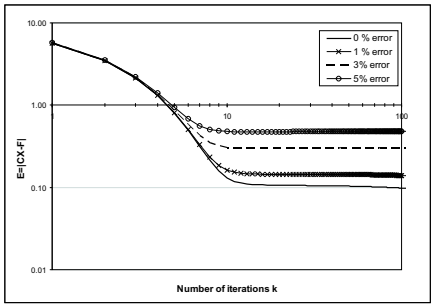

Figure 7: The convergence error $E = \|\mathbf{CX} - \mathbf{F}\|_2$, as a function of the number of iterations, k, obtained using $N = 48$ isoparametric quadratic boundary elements and various amounts of noise added into the input data $\mathbf{u}|_{\Gamma_2}$, namely $p = 0\%(\text{——})$, $p = 1\%(\times)$, $p = 3\%(--)$ and $p = 5\%(\circ)$, for the Cauchy problem considered in Example 1.

displacement and the traction vectors on Γ_2 and it is expected to provide an appropriate stopping criterion. Indeed, if we investigate the error E obtained at every iteration for various levels of Gaussian random noise added into the input displacement data $\widetilde{\mathbf{u}}|_{\Gamma_1}$, we obtain the curves represented graphically in Figure 7. Although more rigorous stopping criteria, such as the discrepancy principle [13] or the generalized cross-validation [14], could have been used, an L-curve type criterion which ceases the iterative procedure at the iteration number, k_{opt}, corresponding to the corner in the curve represented in Figure 7 has been chosen as the stopping criterion, see e.g. Hansen [12]. From Figures 6 and 7 it can be seen that the proposed stopping criterion is very efficient in locating the point where the errors in the numerical solution increase and the iterative process should be terminated.

5.6 Stability of the algorithm

Based on the stopping criterion described in the previous section, the numerical results for the displacement u_1 and the traction t_2 on the underspecified boundary Γ_1, obtained using various levels of noise added into the displacement vector on the boundary Γ_2, for the Example 1, are presented in Figure 8. From this figure it can be seen that the numerical solution is a stable approximation to the exact solution, free of unbounded and rapid oscillations.

6. CONCLUSIONS

In this paper, the Cauchy problem for two-dimensional anisotropic linear elasticity was investigated. In order to deal with the instabilities of the solution of this ill-posed problem, an alternating iterative BEM was employed which reduced the Cauchy problem to solving a sequence of well-posed mixed boundary value problems. A stopping criterion, necessary for ceassing the iterations at the point where the accumulation of noise becomes dominant and the errors in predicting the exact solution increase, has also been presented. The numerical results for various BEM discretisations and various levels of noise added into the input data showed that the BEM produces a convergent, stable and consistent numerical solu-

tion with respect to increasing the number of boundary elements and decreasing the amount of noise. Moreover, the accuracy of the numerical solution has been improved by using a variable relaxation factor.

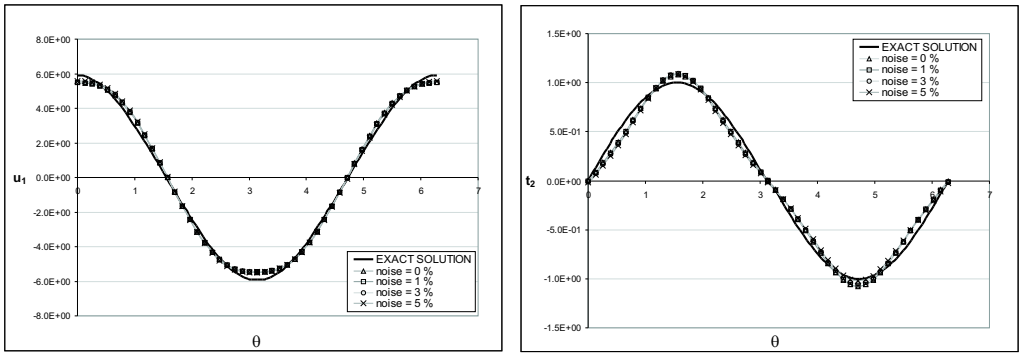

Figure 8: The exact and the numerical solutions for the displacement u_1 (left) and the traction t_2 (right) on the underspecified boundary Γ_1, obtained using $N_e = 48$ elements and various amounts of noise added into input data $\mathbf{u}|_{\Gamma_2}$, for the Example 1.

REFERENCES

1. J. Hadamard, *Lectures on Cauchy Problem in Linear Partial Differential Equations*, Oxford University Press, London, 1923.
2. A. Maniatty, N. Zabaras and K. Stelson, Finite element analysis of some elasticity problems. *Journal of Engineering Mechanics Division ASCE* (1989) **115**, 1302 – 1316.
3. D. Schnur and N. Zabaras, Finite element solution of two-dimensional elastic problems using spatial smoothing. *International Journal for Numerical Methods in Engineering* (1990) **30**, 57 – 75.
4. L. Marin, L. Elliott, D.B. Ingham and D. Lesnic, Boundary element method for the Cauchy problem in linear elasticity. *Engineering Analysis with Boundary Elements* (2001) **25**, 783 – 793.
5. L. Marin, L. Elliott, D.B. Ingham and D. Lesnic, An alternating boundary element algorithm for a singular Cauchy problem in linear elasticity. *Computational Mechanics* (2002) **28**, 479−488. Moscow, 1986.
6. V.A. Kozlov, V.G. Maz'ya and A.F. Fomin, An iterative method for solving the Cauchy problem for elliptic equations. *Computational Mathematics and Mathematical Physics* (1991) **31**, 45 – 52.
7. S.G. Lekhnitskii, *Theory of Elasticity of an Anisotropic Body*, Mir Publishers, Moscow, 1981.
8. F. París and J. Cañas, *Boundary Element Method. Fundamentals and Applications*, Oxford University Press, London, 1997.
9. P. Sollero, *Fracture Mechanics Analysis of Anisotropic Laminates by the Boundary Element Method.* PhD thesis, Wessex Institute of Technology, 1994.
10. L. Comino and R. Gallego, Material constant sensitivity boundary integral equation for anisotropic solids. *International Journal for Numerical Methods in Engineering* (2004) Submitted for publication.
11. N.S. Mera, L. Elliott, D.B. Ingham and D Lesnic, The effect of a variable relaxation factor on the rate of convergence in the Cauchy problem, *Boundary Element Techniques*, (ed M.H. Aliabadi), Queen Mary and Westfield College, University of London, London, 1999, pp.357 – 366.
12. P.C. Hansen, *Rank-Deficient and Discrete Ill-Posed Problems: Numerical Aspects of Linear Inversion*, SIAM, Philadelphia, 1997.
13. V.A. Morozov, On the solution of functional equations by the method of regularization. *Soviet. Math. Dokl.* (1966) **167**, 414 – 417.
14. G.H. Golub, Practical approximate solutions to linear operator equations when the data are noisy. *SIAM Journal on Numerical Analysis* (1977) **14**, 651 – 667.